

NANO EXPRESS

Open Access



# Synthesis and Characterization of Pure Copper Nanostructures Using Wood Inherent Architecture as a Natural Template

Youming Dong<sup>1,2</sup>, Kaili Wang<sup>1</sup>, Yi Tan<sup>1</sup>, Qingchun Wang<sup>3</sup>, Jianzhang Li<sup>1</sup>, Hughes Mark<sup>2</sup> and Shifeng Zhang<sup>1\*</sup>

## Abstract

The inherent sophisticated structure of wood inspires researchers to use it as a natural template for synthesizing functional nanoparticles. In this study, pure copper nanoparticles were synthesized using poplar wood as a natural inexpensive and renewable template. The crystal structure and morphologies of the copper nanoparticles were characterized by X-ray diffraction and field emission scanning electron microscopy. The optical properties, antibacterial properties, and stability of the hybrid wood materials were also tested. Due to the hierarchical and anisotropic structure and electron-rich components of wood, pure copper nanoparticles with high stability were synthesized with *fcc* structure and uniform sizes and then assembled into corn-cob-like copper deposits along the wood cell lumina. The products of nanoparticles depended strongly on the initial OH<sup>-</sup> concentration. With an increase in OH<sup>-</sup> concentration, Cu<sub>2</sub>O gradually decreased and Cu remained. Due to the restrictions inherent in wood structure, the derived Cu nanoparticles showed similar grain size in spite of increased Cu<sup>2+</sup> concentration. This combination of Cu nanostructures and wood exhibited remarkable optical and antibacterial properties.

**Keywords:** Copper nanoparticles, Wood template, Hierarchical structure, Stability

## Background

Metal nanoparticles have garnered wide attention in the scientific community thanks to their exceptional physical and chemical properties [1]. Silver and gold have attracted particularly great interest given their unique plasmon resonance and high stability. However, the high cost of silver and gold limits their wide industrial application [2]. Because copper is much cheaper and more abundant, copper nanoparticles (Cu NPs) may be considered a replacement for silver and gold NPs. Moreover, Cu-based NPs are gaining importance thanks to their catalytic, optical, antibacterial, and electrical conducting properties [3–5]. To fully utilize these properties, the size, purity, and shapes of copper must be well controlled. Therefore, various attempts have been proposed to synthesize NPs with a controlled shape and a specific size distribution, such as solution reduction, thermal decomposition, metal vapor synthesis, radiation methods, microemulsion techniques, mechanical

attrition, and electrodeposition [6–10]. Among these, the solution reduction approach is a feasible and exceptionally versatile method for the preparation of Cu NPs. However, it is common to find nanoparticle molecules with spherical shapes; controlled NPs synthesis with other distinct surface morphologies can be accomplished using some unique organic/inorganic templates [11]. Nevertheless, the template consumption in the preparation process is costly, and the procedure is tedious [12].

Another issue in utilizing these Cu NPs is their inherent propensity for surface oxidation in air and resultant aggregation [13]. To avoid this problem, an inert environment (e. g., nitrogen or argon) is used [14]. Other reports have presented various approaches that attempt to address the oxidation problem; such methods are generally based on minimizing exposure of the Cu NPs to oxygen through a protective layer at the particle surface. This layer may consist of polymers [15], organic ligands [16, 17], carbon and graphene [18], or inert metal [19]; however, these strategies require complex processes and/or special equipment.

Wood can be considered a natural template due to its sophisticated structure. As shown in Fig. 1, wood possesses

\* Correspondence: [shifeng.zhang@bjfu.edu.cn](mailto:shifeng.zhang@bjfu.edu.cn)

<sup>1</sup>MOE Key Laboratory of Wooden Material Science and Application, Beijing Forestry University, Beijing 100083, China

Full list of author information is available at the end of the article

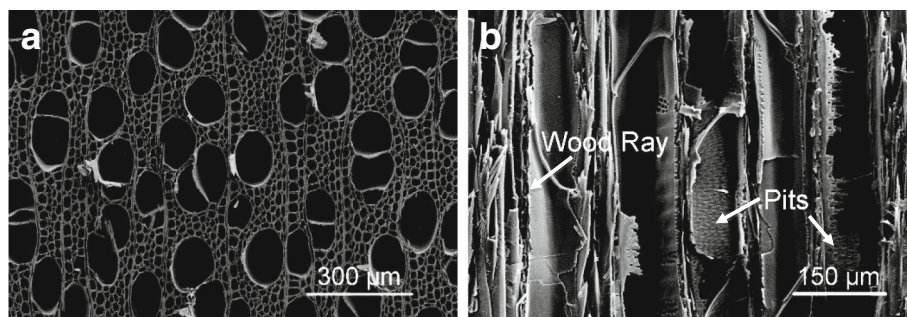


**Fig. 1** Microstructure of poplar wood. **a** Cross section. **b** Longitudinal section

a porous structure from nanoscale to microscale, which provides accessibility to introduce functional materials. Keplinger et al. used wood structure as a mechanically stable scaffold for stimuli responsive gels [20]. Our previous study indicated that wood can be used as the template for assembled ZnO nanostructures [21]. Hybrid wood materials exhibit extraordinary performance in thermal stability, ultraviolet resistance, and antibacterial properties. Due to the inherent hierarchical and anisotropic structure of wood, NP growth within the wood structure is likely to form a 3D order that presents faceted shapes [22]. For instance, magnetic wood with anisotropy can be prepared via coprecipitation of ferric and ferrous ions, and the layered nanosize particles can attach firmly to the inner wood cell wall surface [23]. Therefore, wood is an ideal template to combine with NPs to produce inexpensive, lightweight, and multifunctional materials.

In addition to the unique structure of wood, its lignocellulosic nature—composed of cellulose, lignin, and hemicelluloses—has a reducing and stabilizing effect on metal NPs given the electron-rich features of hydroxyl and phenolic groups in these components [24]. Lin [25, 26] demonstrated that Pt NPs and Ag NPs with a controlled size and shape were successfully synthesized using wood nanomaterials in aqueous systems without employing any other reductants. They attributed the formation of NPs to the reducibility of hydroxyl and phenolic groups in wood components that reduce Pt ions and Ag ions. However, the sophisticated structure of wood has been underused such that

the generated Cu NPs have been susceptible to oxidation in previous studies. Hence, wood components appear to be beneficial to NP stability if the NPs are synthesized using solid wood as a template.

In this study, we reported the success of a novel Cu architecture via chemical reduction within poplar wood as the natural template. The morphologies and crystal structure of the Cu NPs were characterized, and the stability, optical properties, and antibacterial properties of the hybrid wood materials were investigated.

## Methods/Experimental

### Materials

From the sound sapwood portions of poplar (*Populus tomentosa* Carr.), samples with a dimension of  $50 \times 50 \times 5$  (longitudinal)  $\text{mm}^3$  were prepared and oven-dried at  $103^\circ\text{C}$  to a constant weight.

Copper (II) chloride dehydrate ( $\text{CuCl}_2 \cdot 2\text{H}_2\text{O}$ ) and sodium borohydride ( $\text{NaBH}_4$ ) were purchased from Sino-pharm Chemical Reagent Co., Ltd. (Shanghai, China). Other analytical-grade chemical reactants were obtained from Beijing Chemical Reagents Co., Ltd. (Beijing, China).

### Preparation of Wood/Cu Composites

The fabrication process of hybrid wood materials is shown in Fig. 2.  $\text{NaBH}_4$  was used as the reducing agent for  $\text{CuCl}_2 \cdot 2\text{H}_2\text{O}$ . The concentration of the  $\text{NaBH}_4$  and  $\text{CuCl}_2 \cdot 2\text{H}_2\text{O}$  solutions was prepared by adding stoichiometric  $\text{NaOH}$ . Wood samples were dipped in the  $\text{CuCl}_2 \cdot 2\text{H}_2\text{O}$  solution under a vacuum (ca. 0.095 MPa) for

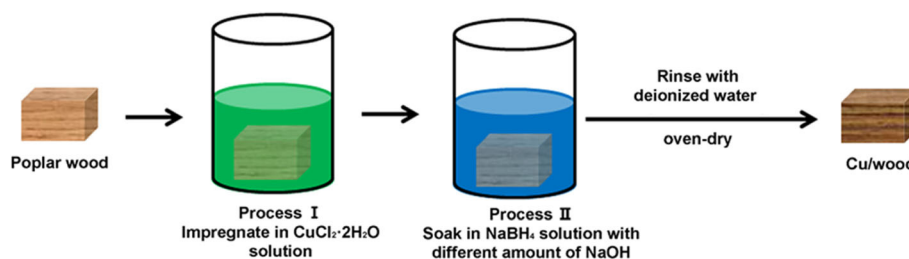


**Fig. 2** Fabrication process of hybrid wood materials

30 min and were soaked under atmospheric pressure for 2 h for in-depth diffusion into the porous wood structure. After impregnation, the samples were rapidly immersed in 200 mL  $\text{NaBH}_4$  solution with different amounts of NaOH for 48 h. The samples were then rinsed with deionized water until the pH value was neutral before being oven-dried at 30 °C for 72 h. Detailed formulations of these solutions are listed in Table 1.

### Characterization of Cu Nanostructures

The X-ray diffraction (XRD) measurements of the NPs were carried out using a Bruker D8 advance diffractometer (Germany). The apparatus parameters were set as follows: Cu-K $\alpha$  radiation with a graphite monochromator, voltage 40 kV, electric current 40 mA, and  $2\theta$  scan range from 5° to 90° with a scanning speed of 2°/min.

The morphologies of Cu nanostructures were examined using a field emission scanning electron microscope (FE-SEM, Hitachi SU8010, Japan) equipped with an energy dispersive X-ray spectroscopy (EDS, EX-350, Horiba Scientific, Japan). The interior portions of longitudinal planes in the sample were mounted on conductive adhesives and were coated with gold sputter followed by observation using FE-SEM at a voltage of 5 kV.

### Evaluation of Optical and Antibacterial Properties

The diffuse reflectance UV-VIS spectra were measured using a UV-VIS spectrophotometer (Cary-300) equipped with an integrating sphere. The scanning range was from 800 to 300 nm.

For bactericidal experiments, the hybrid wood materials were machined into round shape with diameter of 10 mm. The bacterial suspension (*Escherichia coli*) was applied uniformly on the surface of a nutrient agar plate before placing the samples on the plate (1 control and 2 treated samples per plate). The plates were incubated at 37 °C for 24 h, after which the average diameters of the inhibition zone surrounding the samples were measured with a ruler with up to 0.1 mm resolution.

## Results and Discussion

### X-ray Diffraction Analysis

Figure 3a displays the XRD patterns of samples in groups A, B, C, and D. For all samples, obvious

**Table 1** Solution formulations

Groups	$\text{CuCl}_2$ (mol/L)	$\text{NaBH}_4$ (mol/L)	NaOH (mol/L)
A	0.5	0.25	0.5
B	0.5	0.25	0.8
C	0.5	0.25	1.0
D	0.5	0.25	1.2
E	1.0	0.50	1.0
F	1.5	0.75	1.0

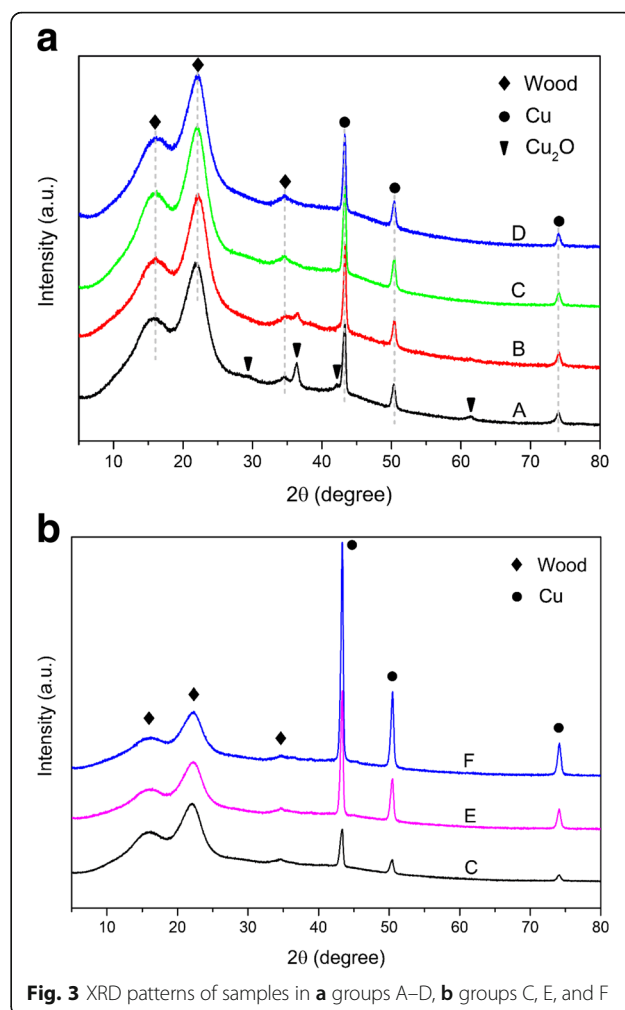


**Fig. 3** XRD patterns of samples in **a** groups A–D, **b** groups C, E, and F

characteristic peaks appearing around 15.9°, 22.1°, and 34.5° were assigned to (101), (002), and (040) planes of cellulose, respectively [27]. The characteristic peaks around 43.3°, 50.4°, and 74.1° were attributed to the (111), (200), and (220) planes of Cu, respectively, which can be indexed to the *fcc* structure of Cu (JCPDS No. 85–1326) [10, 28]. However, some small peaks at around 29.7°, 36.4°, 42.2°, and 61.4° only appeared in samples A and B, associated with the (110), (111), (200), and (220) planes of  $\text{Cu}_2\text{O}$  NPs, respectively [10]. These phenomena indicated that the products of nanoparticles depended strongly on the initial  $\text{OH}^-$  concentration. At a lower concentration, the products were mainly Cu and  $\text{Cu}_2\text{O}$  NPs. As  $\text{OH}^-$  concentration increased,  $\text{Cu}_2\text{O}$  NPs gradually decreased. When the  $\text{OH}^-$  concentration reached 1.0 mol/L or higher, all the  $\text{Cu}_2\text{O}$  contaminants disappeared and only Cu NPs remained in the products. Generally, the metallic Cu can be synthesized through redox reaction between  $\text{Cu}^{2+}$  and  $\text{NaBH}_4$  [29]. The presence of  $\text{OH}^-$  in this system

is to adjust the pH and accelerate the reaction in water [30].  $\text{NaBH}_4$  could react with  $\text{H}_2\text{O}$  when pH is below 9.5, which will weaken its reducing capacity [31]. Therefore, the pH was adjusted to 10–12 by NaOH [5]. In addition, the grain size of Cu NPs will be decreased with the increase in pH value [31]. However, wood components are sensitive to the high alkaline condition and are degraded by NaOH, which will reduce the concentration of  $\text{OH}^-$ . Thus, higher concentration of  $\text{OH}^-$  was needed to synthesize pure Cu NPs in wood template. At high  $\text{OH}^-$  concentration,  $\text{Cu}^{2+}$  was transformed to  $\text{Cu}(\text{OH})_2$  as precursor, then reduced by  $\text{NaBH}_4$ , which could be confirmed from the solution color change from deep blue to colorless [32]. However, the transition of metal Cu cannot usually be obtained via the reduction of simple Cu salts without other reagents such as protective polymers with functional groups. Instead, the reduction is more likely to stop at the  $\text{Cu}_2\text{O}$  stage due to the presence of a large number of water molecules [33]. In this case, the generation of pure Cu NPs may have been due to the wood template: firstly, the hierarchical structure of wood contributed to the assembly of NPs; and secondly, the electron-rich features of phenolic and hydroxyl groups in wood components exerted a reducing and stabilizing effect on Cu NPs [25].

To study the effect of  $\text{Cu}^{2+}$  concentration on the products, XRD patterns of samples in groups C, E, and F are shown in Fig. 3b. As the  $\text{Cu}^{2+}$  concentration gradually increased, the intensity of Cu crystal diffraction peaks increased accordingly, indicating that more Cu NPs were generated in the wood template. The

**Table 2** The grain size of Cu NPs in group C, E, and F

Groups	Grain size (nm)		Significance <sup>a</sup>
	Initial synthesis	After storage	
C	$19.54 \pm 1.87$	$18.34 \pm 1.59$	NS <sup>b</sup>
E	$19.74 \pm 2.41$	$18.93 \pm 1.18$	NS
F	$21.36 \pm 3.09$	$20.08 \pm 1.76$	NS

<sup>a</sup>One-way analysis of variance at  $\alpha = 0.05$

<sup>b</sup>NS means not significant

crystallite size was calculated using the Scherrer equation,

$$D = \frac{K\lambda}{\beta \cos\theta}$$

where  $D$  is the crystallite size,  $k$  is Scherrer constant (= 0.94 assuming that the particles are spherical),  $\lambda$  is the wavelength of the X-ray radiation (0.15418 nm),  $\beta$  is the full width of the peak at half maximum, and  $\theta$  is the diffraction angle [10].

The average diameter of Cu NPs was calculated according to the peaks of (110), (200), and (220). The average grain size of Cu NPs in samples C, E, and F were estimated to be approximately 19.5, 19.7, and 21.3 nm, respectively (Table 2). Although the concentration of  $\text{Cu}^{2+}$  increased significantly, the derived Cu NPs exhibited similar grain size, possibly because the hierarchical structure of wood restricts the growth of Cu NPs [34].

After being stored for 1 year in ambient conditions, the stability and grain sizes of Cu NPs in the wood samples were evaluated. Figure 4 displays the XRD patterns of samples in groups C, E, and F. The main signals of Cu

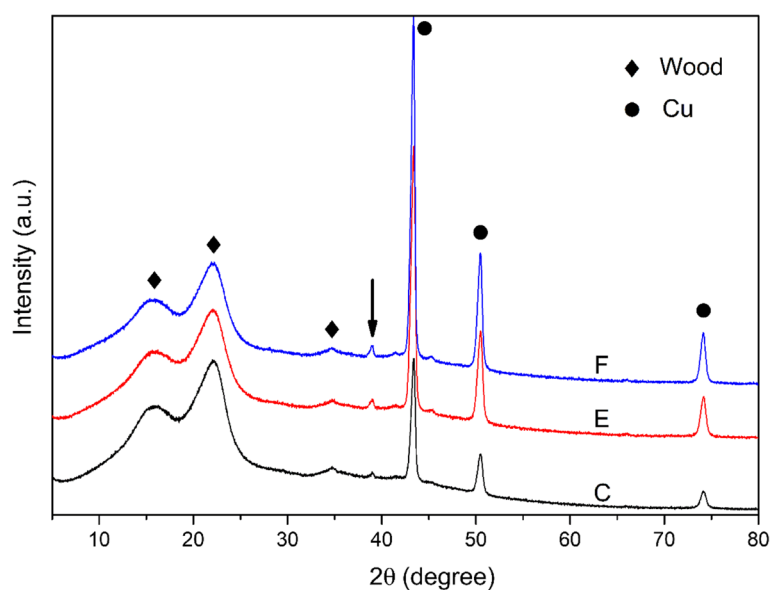
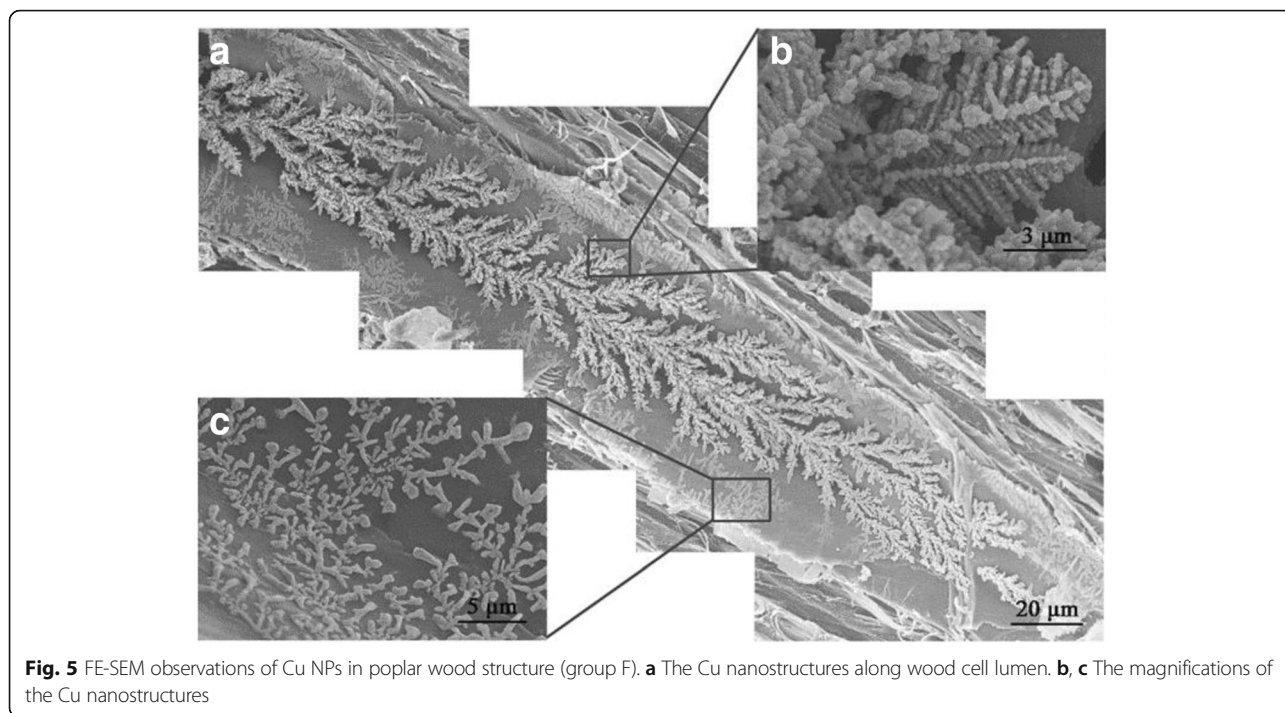


**Fig. 4** XRD patterns of groups C, E, and F after 1 year stored in ambient conditions

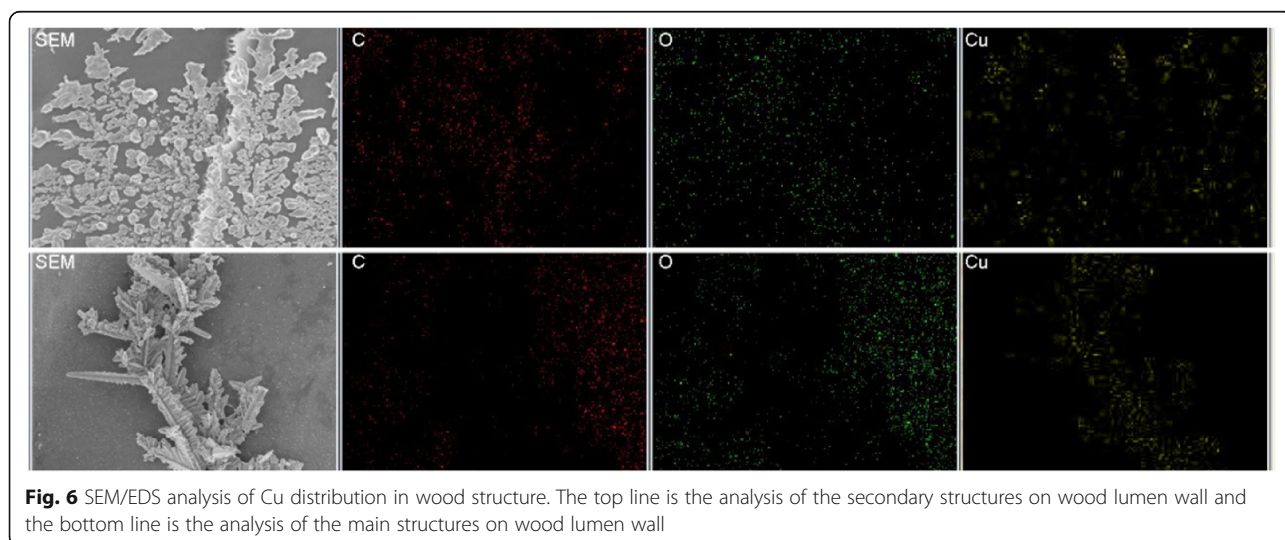


NPs in the wood samples were similar to those shown in Fig. 3; only the small peak appearing at 38.9° could be related to the CuO (see arrow in Fig. 4). From Table 2, the average grain size of Cu NPs in samples C, E, and F were similar to the initial sizes. There was no significant change after storage according to the one-way analysis of variance. These results indicated high stability of Cu NPs in the wood structure. Therefore, the problems of oxidation and aggregation could be circumvented by the use of wood templates, presumably due to the protective effect of the wood's original structure and components. In

addition, the oxidation layer on the wood surface may also contribute to the stability of the internal Cu NPs.

**Morphology Analysis**

The morphology of Cu nanostructures was assessed via FE-SEM; all samples exhibited a similar assembled structure and morphology of Cu nanostructures, as shown in Fig. 5. In Fig. 5a, the agglomerates exhibited a 3D structure along the wood cell lumina that consisted of corncob-like deposits. In addition, many secondary structures adhered to the walls of the cell lumina. Figure 5b, c displays the



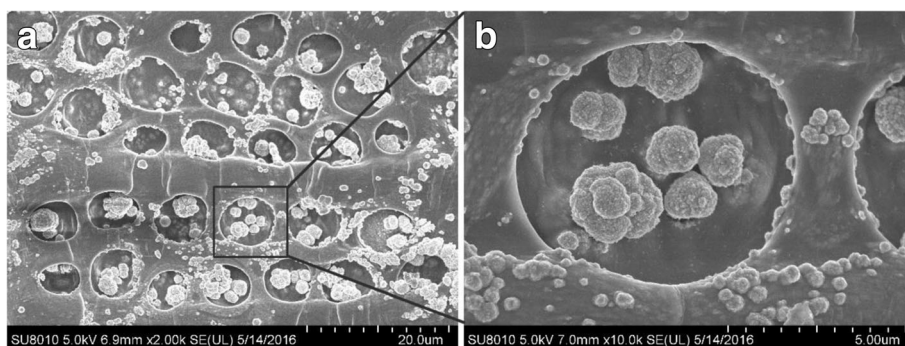


**Fig. 7** FE-SEM observations of Cu NPs in pits of wood (group F). **a** 2k magnification, **b** 10k magnification

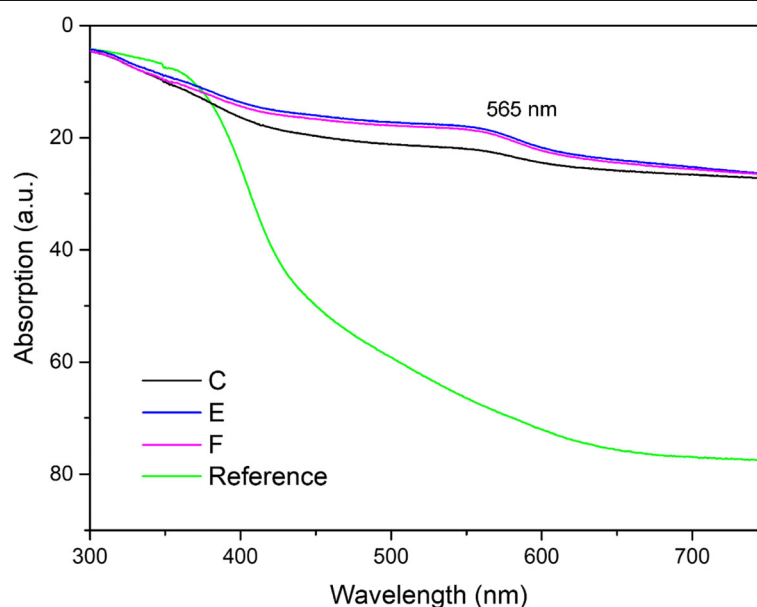
magnifications of the structures. The pristine wood cell lumen wall was smooth as shown in Fig. 1b. Therefore, the agglomerates on the cell lumen wall could be the assembly of Cu NPs, confirmed by the EDS analysis (Fig. 6). Due to wood's anisotropic structure, the assembly was oriented, which could explain the anisotropic properties of the materials [23].

Figure 7 shows the FE-SEM observation of nanostructures in pit of wood. In contrast to that in cell lumen, the Cu NPs in pits were assembled into small spherical agglomerates with diameter from 1 to 2.5  $\mu\text{m}$ . From the magnified image in Fig. 7b, more smaller agglomerates with diameter  $< 500$  nm were adhered to the wall of pit structure. These small and spherical agglomerates could be attributed to the inhibition effect of wood pit structures. It was possible to utilize the wood's inherent architecture to synthesize the NPs and influence crystallization to some extent, where the NPs no longer

resembled the commonly encountered morphologies obtained from classical precipitation reactions in the absence of templates. On the other hand, poplar wood could be endowed with the catalytic, optical, antimicrobial, and electrical conducting properties of Cu NPs, which would expand wood applications. Previous research has suggested that most Cu NPs are too large to penetrate the wood structure, and their distribution is uneven. Nonetheless, this method could provide a potential approach for fabricating a uniform hybrid wood material via in situ chemosynthesis.

#### Optical and Antibacterial Properties

Figure 8 shows the UV-vis diffuse reflectance curves of the original and hybrid wood materials. The absorption intensity of the hybrid wood materials was higher than that of the control samples. The absorption maxima reached 565 nm for the hybrid wood materials, which



**Fig. 8** UV-Vis spectra of original wood and hybrid wood materials

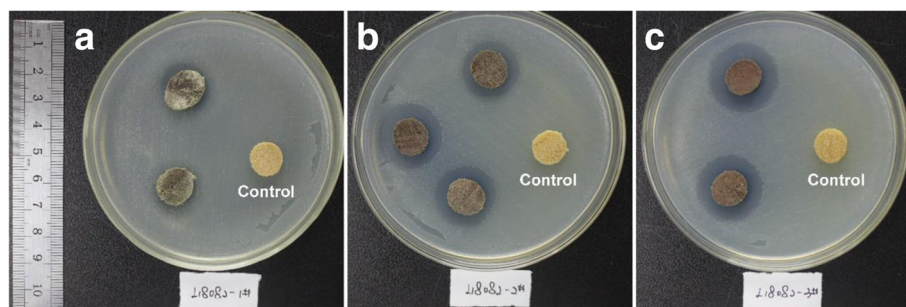


**Fig. 9** Antibacterial testing of original wood and hybrid wood materials. **a** Group C. **b** Group E. **c** Group F

was more remarkable in groups E and F due to the higher amount of Cu NPs. This result concurred with the reported plasmon band of dark red Cu NPs in the 560 to 570 nm range [35]. From Fig. 9, in contrast to the control, treated samples in all groups clearly showed zones of inhibition, indicating an antibacterial property against *Escherichia coli*. The average widths of the inhibition zone were 0, 3.2, 4.8, and 6.2 mm for control, groups C, E, and F, respectively. Apparently, the antibacterial property was increased with the increase in the concentration of Cu NPs in wood samples. These results indicated that the incorporation of Cu NPs endowed wood with high antibacterial properties. Thus, the incorporation of Cu NPs can provide wood with optical and antibacterial properties, and other potential properties (e.g., UV resistance as reported in [36]) could also be introduced.

## Conclusions

To leverage the inherent hierarchical, anisotropic architecture, and electron-rich components of wood, pure Cu NPs were derived with unique shapes and sizes through wood template methods. The Cu NPs exhibited a 3D structure along the wood cell lumina that consisted of corn-cob-like Cu deposits. The nanoparticle products depended strongly on the initial  $\text{OH}^-$  concentration. With an increase in  $\text{OH}^-$  concentration,  $\text{Cu}_2\text{O}$  gradually decreased and Cu remained. As the  $\text{Cu}^{2+}$  concentration increased gradually, more Cu NPs were generated in the wood structure. The assembled structure of NPs invariably exhibited corn-cob-like Cu deposits in the wood templates. Due to the unique structure and components of wood, the oxidation and aggregation of Cu NPs could be circumvented. Additionally, this new hybrid wood material, combined with the advantages of wood and Cu nanostructures, exhibited remarkable optical and antibacterial properties.

## Acknowledgements

The authors are very grateful for the support from the China Scholarship Council (CSC).

## Funding

This work was supported by the Fundamental Research Funds for the Central Universities (no. 2016ZCQ01) and the National Natural Science Foundation of China (Project 51779005/E090301).

## Availability of Data and Materials

The datasets generated during and/or analyzed during the current study are available from the corresponding authors on reasonable request.

## Authors' Contributions

YD, KW, YT, and QW conducted the experiments and gathered the data. SZ, HM, and JL conceived and supervised the work. YD analyzed the data and prepared the manuscript. All authors read and approved the final manuscript.

## Competing Interests

The authors declare that they have no competing interests.

## Publisher's Note

Springer Nature remains neutral with regard to jurisdictional claims in published maps and institutional affiliations.

## Author details

<sup>1</sup>MOE Key Laboratory of Wooden Material Science and Application, Beijing Forestry University, Beijing 100083, China. <sup>2</sup>Wood Material Technology, Department of Bioproducts and Biosystems, School of Chemical Engineering, Aalto University, 02150 Espoo, Finland. <sup>3</sup>School of Technology, Beijing Forestry University, Beijing 100083, China.

Received: 4 January 2018 Accepted: 17 April 2018

Published online: 24 April 2018

## References

- Perelaer J, Smith PJ, Mager D, Soltman D, Volkman SK, Subramanian V et al (2010) Printed electronics: the challenges involved in printing devices, interconnects, and contacts based on inorganic materials. *J Mater Chem* 20:8446–8453
- Tsai CY, Chang WC, Chen GL, Chung CH, Liang JX, Ma WY et al (2015) A study of the preparation and properties of antioxidative copper inks with high electrical conductivity. *Nanoscale Res Lett* 10:357
- Dayakar T, Rao KV, Bikshalu K, Rajendar V, Park SH (2017) Novel synthesis and characterization of pristine Cu nanoparticles for the non-enzymatic glucose biosensor. *J Mater Sci Mater Med* 28:109
- Cheirnadurai K, Biswas S, Murali R, Thanikaivelan P (2014) Green synthesis of copper nanoparticles and conducting nanobiocomposites using plant and animal sources. *RSC Adv* 4:19507–19511
- Zhang HX, Siegert U, Liu R, Cai WB (2009) Facile fabrication of ultrafine copper nanoparticles in organic solvent. *Nanoscale Res Lett* 4:705–708
- Kumar A, Saxena A, De A, Shankar R, Mozumdar S (2013) Facile synthesis of size-tunable copper and copper oxide nanoparticles using reverse microemulsions. *RSC Adv* 3:5015–5021

7. Gawande MB, Goswami A, Felip FX, Asefa T, Huang X, Silva R et al (2016) Cu and Cu-based nanoparticles: synthesis and applications in catalysis. *Chem Rev* 116:3722–3811
8. Ramyadevi J, Jeyasubramanian K, Marikani A, Rajakumar G, Rahuman AA (2012) Synthesis and antimicrobial activity of copper nanoparticles. *Mater Lett* 71:114–116
9. Nam D, Kim R, Han D, Kim J, Kwon H (2011) Effects of  $(\text{NH}_4)_2\text{SO}_4$  and BTA on the nanostructure of copper foam prepared by electrodeposition. *Electrochim Acta* 56:9397–9405
10. Salavati-Niasari M, Davar F (2009) Synthesis of copper and copper (I) oxide nanoparticles by thermal decomposition of a new precursor. *Mater Lett* 63:441–443
11. Zhang QL, Yang ZM, Ding BJ, Lan XZ, Guo YJ (2010) Preparation of copper nanoparticles by chemical reduction method using potassium borohydride. *Trans Nonferrous Metals Soc China* 20:s240–s244
12. Xu C, Nie D, Chen H, Wang Y, Liu Y (2015) Template-free synthesis of magnetic CoNi nanoparticles via a solvothermal method. *Mater Lett* 138:158–161
13. Magdassi S, Grouchko M, Kamysnyy A (2010) Copper nanoparticles for printed electronics: routes towards achieving oxidation stability. *Materials* 3:4626–4638
14. Umer A, Naveed S, Ramzan N, Rafique MS (2012) Selection of a suitable method for the synthesis of copper nanoparticles. *Nano* 7:1230005
15. Pulkkinen P, Shan J, Leppänen K, Käsäkoski A, Laiho A, Järn M et al (2009) Poly (ethylene imine) and tetraethylenepentamine as protecting agents for metallic copper nanoparticles. *ACS Appl Mater Interface* 1:519–525
16. Mott D, Galkowski J, Wang L, Luo J, Zhong CJ (2007) Synthesis of size-controlled and shaped copper nanoparticles. *Langmuir* 23:5740–5745
17. Raza A, Javed S, Qureshi MZ, Khan MU, Khan MS (2017) Synthesis and study of catalytic application of L-methionine protected gold nanoparticles. *Appl Nanosci* 7:429–437
18. Luechinger NA, Athanassiou EK, Stark WJ (2008) Graphene-stabilized copper nanoparticles as an air-stable substitute for silver and gold in low-cost ink-jet printable electronics. *Nanotechnol* 19:445201
19. Cazayous M, Langlois C, Oikawa T, Ricolleau C, Sacuto A (2006) Cu-Ag core-shell nanoparticles: a direct correlation between micro-Raman and electron microscopy. *Phys Rev B* 73:113402
20. Keplinger T, Cabane E, Berg JK, Segmehl JS, Bock P, Burgert I (2016) Smart hierarchical bio-based materials by formation of stimuli-responsive hydrogels inside the microporous structure of wood. *Adv Mater Interface*:3. <https://doi.org/10.1002/admi.201600233>
21. Dong Y, Yan Y, Ma H, Zhang S, Li J, Xia C et al (2017) In-situ chemosynthesis of ZnO nanoparticles to endow wood with antibacterial and UV-resistance properties. *J Mater Sci Technol* 33:266–270
22. Trey SM, Olsson RT, Strom V, Berglund LA, Johansson M (2014) Controlled deposition of magnetic particles within the 3-D template of wood: making use of the natural hierarchical structure of wood. *RSC Adv* 4:35678–35685
23. Merk V, Chanana M, Gierlinger N, Hirt AM, Burgert I (2014) Hybrid wood materials with magnetic anisotropy dictated by the hierarchical cell structure. *ACS Appl Mater Interface* 6:9760–9767
24. Benaisi K, Johnson L, Walsh DA, Thielemans W (2010) Synthesis of platinum nanoparticles using cellulosic reducing agents. *Green Chem* 12:220–222
25. Lin X, Wu M, Wu D, Kuga S, Endo T, Huang Y (2011) Platinum nanoparticles using wood nanomaterials: eco-friendly synthesis, shape control and catalytic activity for *p*-nitrophenol reduction. *Green Chem* 13:283–287
26. Lin X, Wang F, Kuga S, Endo T, Wu M, Wu D et al (2014) Eco-friendly synthesis and antibacterial activity of silver nanoparticles reduced by nano-wood materials. *Cellulose* 21:2489–2496
27. Cave I (1997) Theory of X-ray measurement of microfibril angle in wood. *Wood Sci Technol* 31:225–234
28. Kou J, Saha A, Bennett-Stampfer C, Varma RS (2012) Inside-out core-shell architecture: controllable fabrication of  $\text{Cu}_2\text{O}@\text{Cu}$  with high activity for the Sonogashira coupling reaction. *Chem Commun* 48:5862–5864
29. Glavee GN, Klabunde KJ, Sorensen CM, Hadjipanayis GC (1994) Borohydride reduction of nickel and copper ions in aqueous and nonaqueous media. Controllable chemistry leading to nanoscale metal and metal boride particles. *Langmuir* 10:4726–4730
30. Dang TMD, Le TTT, Fribourg-Blanc E, Dang MC (2011) Synthesis and optical properties of copper nanoparticles prepared by a chemical reduction method. *Adv Nat Sci Nanosci Nanotechnol* 2:015009
31. Liu QM, Zhou DB, Yamamoto Y, Ichino R, Okido M (2012) Preparation of Cu nanoparticles with  $\text{NaBH}_4$  by aqueous reduction method. *Trans Nonferrous Met Soc China* 22:117–123
32. Liu QM, Zhou DB, Yamamoto Y, Kuruda K, Okido M (2012) Effects of reaction parameters on preparation of Cu nanoparticles via aqueous solution reduction method with  $\text{NaBH}_4$ . *Trans Nonferrous Met Soc China* 22: 2991–2996
33. Qi L, Ma J, Shen J (1997) Synthesis of copper nanoparticles in nonionic water-in-oil microemulsions. *J Colloid Interface Sci* 186:498–500
34. Li A, Jin Y, Muggli D, Pierce DT, Aranwela H, Marasinghe GK et al (2013) Nanoscale effects of silica particle supports on the formation and properties of  $\text{TiO}_2$  nanocatalysts. *Nano* 5:5854–5862
35. Kanninen P, Johans C, Merta J, Kontturi K (2008) Influence of ligand structure on the stability and oxidation of copper nanoparticles. *J Colloid Interface Sci* 318:88–95
36. Gascón-Garrido P, Mainusch N, Millitz H, Viöl W, Mai C (2017) Copper and aluminium deposition by cold-plasma spray on wood surfaces: effects on natural weathering behaviour. *Eur J Wood Prod* 75:315–324

Submit your manuscript to a SpringerOpen® journal and benefit from:

- Convenient online submission
- Rigorous peer review
- Open access: articles freely available online
- High visibility within the field
- Retaining the copyright to your article

---

Submit your next manuscript at ► [springeropen.com](http://springeropen.com)

---